Miniaturized Fiber-top Cantilevers on Etched Fibers

CAMIEL H. VAN HOORN,[1] MOXI CUI,[1] DAVIDE IANNUZZI[1*]

[1]Department of Physics and Astronomy and LaserLab Amsterdam, VU University, Amsterdam, The Netherlands

**Corresponding author: d.iannuzzi@vu.nl*

Abstract: Fiber-top probes are self-aligned, all optical devices obtained by carving a cantilever on top of a 125 µm diameter single-mode optical fiber. In this paper, we show that this design can be adapted to smaller fibers as well. We evaluated the performance of a 20 µm diameter probe in contact mode atomic force microscopy (AFM) and that of a 50 µm diameter probe in nano-indentation measurements. AFM images proved to be accurate both in air and water, although some distortion was observed because of the mechanical bending of the fiber during scanning. Indentation curves resembled those obtained with larger devices. The maximum indentation depth, however, is limited by the small dimensions of the cantilever.

Key words: *Fiber optics; Scanning microscopy; Fiber optics sensors;*

Since its invention in 1986 (Binnig, 1986), the atomic force microscope (AFM) has been recognized as a valuable tool for nanoscale imaging and material characterization (Jalili & Laxminarayana, 2004). In 2006, a new kind of AFM probe was proposed that could eliminate the burden of the optical triangulation alignment, minimizing the effects of thermal drifts, and reducing the complexity incurred when dealing with samples immersed in liquids: the

fiber-top cantilever (Iannuzzi[1] *et al.*, 2006 and Iannuzzi[2] *et al*., 2006). The idea behind this approach gravitates around the possibility of carving the cleaved end of an optical fiber in the form of a cantilever, which, by design, is aligned with the core of the fiber. The cantilever and the end of the fiber together form the two mirrors of a Fabry-Perot (FP) cavity, giving the user the opportunity to detect the deflection of the cantilever by coupling light into the proximal end of the fiber and measuring the amount of light reflected back by the cavity. One of the distinctive features of this kind of probes is their unique form factor – a 125 µm diameter wire. One may then ask whether it is possible to fabricate similar devices on even smaller fibers. Smaller probes may have applications where there is a need to characterize an object contained in a volume that is accessible only via a narrow aperture, such as, for instance, a cell inside a porous material (Discher *et al*., 2009). To answer this question, we present here a new set of fiber-top probes fabricated on the tip of an etched fiber. After introducing the fabrication technique, we show the results obtained in contact mode AFM imaging and in indentation mode. We demonstrate that the performance of the new probe is similar to that of larger devices, although some limitations for certain applications may be difficult to overcome.

Fig. 1 illustrates the procedure followed to fabricate the fiber-top cantilevers used in this work. A single mode optical fiber is first immersed into an etchant solution ($HF:NH_4F:H_2O$=1:7:1), which etches the cladding of the fiber at a rate of approximately 0.2 µm/minute. The etched fiber is then mounted inside a focused ion beam (FIB) machine. Here, the fiber end is first machined in the form of a thin ridge (Fig. 1(b)). The base of the bridge is designed to have a 45° slope, in order to avoid unwanted light reflections. The ridge is then machined in the shape of a cantilever, equipped, at its free hanging end, with either a flat punch as shown in Fig. 1(c) or with a sharp pyramidal tip as discussed later in the text. After coating the entire device with a thin layer of metal to make sure that

the bottom of the cantilever is reflective, the fiber is mounted again in the FIB machine to remove the metal from the core of the fiber underneath the cantilever (fig. 1(d)). A typical cantilever has dimensions of 15-45 μm in length, 5-7 μm in width, and 1-2 μm in thickness. The distance of the gap between the fiber end and the cantilever is about 10 μm, whereas the length of the anchoring point is approximately equal to 5 μm.

To detect the deflection of the cantilever, the proximal end of the probe is connected to a commercial readout (OP1550, Optics11). The readout is equipped with a 20 mW tunable laser whose wavelength can be adjusted in the range between 1528 nm and 1563 nm. Neglecting multiple reflections, the light intensity reflected back from the fiber-cantilever FP cavity is given by (Iannuzzi[2] *et al*., 2006, Rugar *et al*., 1989):

$$I(d) = I_f + I_b + 2\sqrt{I_f I_b}\cos(4\pi d/\lambda + \phi_0) \quad (1)$$

where d is the distance between the fiber end and the cantilever, λ is the wavelength of the laser, ϕ_0 is a phase shift that depends on the geometry of the cavity, and I_f and I_b represent the light intensities that one would measure if the reflected beam did not interfere. Clearly, measuring I, one can obtain d.

To demonstrate that this proposed approach works according to design, we first tested one of our miniaturized fiber-top cantilevers in AFM imaging mode (see Fig. 2). For this purpose, the probe (cantilever's dimensions = 15 μm × 5 μm × 1 μm, stiffness ~ 25 N/m), which was fabricated on a 20 μm diameter etched fiber (SMF28, Corning, mode field diameter = 10.4±0.5 μm at 1550 nm) and equipped with a sharp pyramidal tip, was anchored to a translation stage consisting of a vertical piezoelectric actuator (AE0203D04F, Thorlabs Inc.) and a 30 μm × 30 μm range XY-scanner (ANSxy50,

Attocube AG). The probe was then used to image, in closed loop contact mode, a test sample consisting of 20 nm high SiO_2 square plateaus and 1 nm deep square wells on a flat Si wafer (TGQ1, NT-MDT). To emphasize the possibility of gathering images inside small apertures, the sample was mounted at the bottom of a 1 mm high chamber accessible from the top via a 100 µm × 100 µm hole. To reduce acoustic and seismic noise, the entire assembly was mounted on an active vibration isolation stage (Nano-20, Accurion GmbH) housed inside an anechoic box.

At the start of the experiment, the fiber-top probe was first moved through the small aperture of the chamber containing the sample and lowered to push the tip of the cantilever on the sample. The interference signal was used as an input for the feedback loop to keep the bending of the cantilever constant throughout the measurement. The voltage applied to the vertical actuator maintained this position while the raster data acquired over the sample were converted into an image, as in standard closed loop contact mode AFMs.

Fig. 3 shows 10 µm × 10 µm images (256 × 256 pixels) of the sample obtained with the method described above at a scanning speed of 500 nm/s, both in air (a, b) and water (c), along with an image of the grating obtained in air using a commercial AFM in contact mode (NT-MDT) (d). Clearly, both in air and in water, our measured images show the main features of the sample (the 20 nm high squares); the noise level is however too high to neatly distinguish the 1 nm deep wells. In terms of absolute values, in fact, the RMS noise level, measured on a flat part of the sample, is equal to 0.8 nm in air and 2.1 nm in water. This is comparable with previous results reported in fiber-top AFM imaging (Iannuzzi[2] *et. al.*, 2006). One can further notice that the images obtained with our miniaturized probe are affected by a certain degree of distortion. This distortion is most likely due to bending of the thin body of the fiber during scanning, as one can confirm by comparing the trace

and re-trace images (Fig. 3(b)). To exclude that the distortion be due to torque induced motions of the cantilever, we have further collected images with different fast-scanning directions, which, indeed, did not result in the changes of the distortion pattern that one would expect in the presence of torques. The problem, which certainly limits the overall lateral resolution of the probe, could be partially solved by using a softer cantilever or by imaging in tapping-mode. Because the resonant frequency of the cantilever is about 2 MHz, however, tapping mode is not possible with our current setup.

In contact mode AFM imaging, the deflection of the cantilever does not change during the measurement. This is not the case in indentation mode, where the cantilever often needs to deflect over several hundreds of nm before one can calculate the Young modulus of the indented sample. When the cantilever bends, the amount of light reflected back by the cantilever into the fiber changes, giving rise to a change in the visibility of the interference fringes. For small deflection angles (like with standard fiber-top cantilevers), this problem is negligible. However, for miniaturized cantilevers, the decrease of the interference contrast can compromise the measurement. To minimize this problem, we decided to modify our design following the guidelines reported here below:

(1) We decided to fabricate the device out of a high numerical aperture (NA) fiber (UHNA3 Thorlabs). The mode-field diameter of the high NA fiber is 4.0±0.3 μm at a wavelength of 1550 nm.

(2) We increased the diameter of the fiber from 20 μm to 50 μm, and, hence, the length of the cantilever from 15 μm to 45 μm (while keeping the other dimensions similar to the previous probe, i.e., width = 5-7 μm and thickness = 1-2 μm), which corresponds to a decrease of the bending angle for a certain cantilever deflection. The stiffness of the new cantilever can range from 1 to 15 N/m.

(3) We fabricated the cantilever with a 3° initial angle with respect to the fiber facet, which allowed us to double the available deflection range (from -3° to +3°).

To demonstrate that our new miniaturized device can now properly function in indentation mode, we equipped it with a flat punch (see Fig. 1). Considering the similarity of refractive index between glass and water, we coated the fiber end surface with a semitransparent gold layer (15 nm thick) to increase the contrast between the interference fringes. We then attached it onto a piezoelectric actuator, which was mounted, as illustrated in Fig. 4. We first positioned the cantilever in close proximity with a test sample – a small block of PDMS, anchored to a glass slide. To minimize adhesion forces the measurements were carried out in a droplet of water. Driving the piezoelectric actuator with a 2 Hz periodic triangular signal, we were able to repeatedly bring the tip of the cantilever in and out of contact with the sample. Measuring the deflection of the cantilever during the indentation stroke, it was possible to assess the Young modulus of the indented material, as with standard AFMs.

Before analyzing the results, it is important to emphasize that, because the readout scheme is based on interferometry, the output of the readout unit does not scale linearly with d, as clearly indicated in Eq. (1). To solve this problem, one can add a fast oscillating sinusoidal signal (3 kHz, in our case) on top of the slow triangular voltage used to drive the piezoelectric actuator, and send the readout output to a lock-in amplifier locked at the oscillating frequency. The data acquisition process follows a method similar to the one described in the literature (see, for example, van Hoorn *et al*., 2016, and references therein). The output of the readout, which will be hereafter called S_{DC}, follows Eq. (1). On the contrary, the signal at the exit of the lock-in amplifier, which will be hereafter called S_{LI}, provides the first derivative of S_{DC}. In other words, S_{DC} and S_{LI} are proportional to the sine and the cosine of the

same angle. Hence, as the indentation stroke progresses, plotting S_{LI} as a function of S_{DC}, one obtains an elliptical pattern, which can be converted to a unitary circle after a simple axis renormalization. At every specific moment of the indentation, the deflection of the cantilever can be inferred by looking at the angle between the x-axis of the normalized reference frame and the line that goes from the center of the normalized reference frame to the point on the circle that the two signals generate in that specific moment. In other words, the cantilever displacement can then be obtained from phase of the unitary circle (see, for example, van Hoorn *et al*., 2016, and references therein).

Fig. 5 shows the results obtained. Fig. 5(a) and 5(b) show the two signals S_{DC} and S_{LI}, respectively. Fig. 5(c) shows the unitary circle obtained from the previous two graphs. It is to note that the circle does not close on itself perfectly. This phenomenon can be ascribed to the fact that the coupling loss due to bending of the cantilever (Eq. (2)) was still not fully suppressed. Yet, as illustrated in Fig. 5(d), the signals are sufficiently accurate to provide a clear indentation curve. Note that, to go from Fig. 5(c) to Fig. 5(d), we first had to calibrate the probe to infer the relation between the interferometric readout signal at the position of the core of the fiber and the vertical movement at end of the cantilever. For this reason, before measuring on the PDMS sample, we indented a rigid sample, for which one can assume that the indentation depth is zero throughout the entire indentation stroke.

The measured displacement of the cantilever, compared with the movement of the piezoelectric actuator, allows us to calculate the indentation depth and, thus, derive the load-indentation curve, which is reported in Fig. 6. The Young modulus of the sample can be then derived by means of the Oliver and Pharr method (Oliver & Pharr, 1992):

$$\left(dP/dh\right)_{max} = 2\pi^{1/2} \; E \; A^{1/2} \tag{2}$$

where $(dP/dh)_{max}$ is the maximum slope of the pull-out curve, A is the contact area of the flat punch of the tip, and E is the Young modulus of the sample. Assuming that the spring constant of the cantilever is equal to 13 N/m (as calculated from the geometrical dimensions), using Oliver and Phar method we obtained a Young modulus of 2.8 ± 0.1 MPa. This number is in agreement with the value obtained with an independent measurement performed with a commercial ferrule-top instrument (Piuma, Optics11 B.V.).

In conclusion, we have demonstrated that it is possible to fabricate fiber-top cantilevers on etched fibers. These probes provide AFM contact mode images and indentation curves similar to those observed with larger devices. However, miniaturization of the fiber-top technique comes with some limitations, including possible image distortions in contact mode AFM imaging, inadequate mechanical properties of the probe for tapping and non-contact mode AFM imaging, restricted indentation range during AFM testing of the mechanical properties of a sample, limited possibilities to further decrease the spring constant for indentation of ultrasoft samples, and high cost of manufacturing.

The authors thank H. Zeijlemaker for discussions. This work is part of the research programme of the Foundation for Fundamental Research on Matter (FOM), which is financially supported by the Netherlands Organisation for Scientific Research (NWO), and was partially supported by the European Research Council under the European Union's Seventh Framework Programme (FP/2007-2013) / ERC grant agreement n. 615170.

Declaration of interest: DI is shareholder of Optics11 B.V.

Reference

Binnig, G. Quate, C.F. and Gerber, Ch. (1986) Atomic Force Microscope, Physics Review Letters 56, 930-933

Discher, D. *et al*, (2009) Biomechanics: Cell Research and Applications for the Next Decade, Annals of Biomedical Engineering 37, 847-859

Iannuzzi[1], D. Deladi, S. Berenschot, J.W. de Man, S. Heeck, K. and Elwenspoek, M.C. (2006) Fiber-top atomic forcé microscope, Review of Scientific Instruments 77, 106105

Iannuzzi[2], D. Deladi, S. Gadgil, V.J. Sanders, G.P. Schreuders, H. and Elwenspoek, M.C. (2006) Monolithic fiber-top sensor for critical environments and standard applications, Applied Physics Letters 88, 053501

Jalili, N. and Laxminarayana, K. (2004) A review of atomic force microscopy imaging systems: application to molecular metrology and biological sciences, Mechatronics, 14, 907-945

Oliver, W.C. and Pharr, G.M. (1992) An improved technique for determining hardness and elastic modulus using load and displacement sensing indentation experiments, Journal of Materials Research 7, 1564-1583

Rugar, D. Mamin, H.J. and Guethner, P. (1989) Improved fiber-optic interferometer for atomic force microscopy, Applied Physics Letters 55, 2588

Van Hoorn, H., Kurniawan, N. A., Koenderink, G. H. and Iannuzzi, D. (2016) Local dynamic mechanical analysis for heterogeneous soft matter using ferrule-top indentation, Soft Matter, 12, 3066-3073

Captions:

Fig. 1. Illustration of the most relevant steps of the fabrication process: (a) a fiber is first etched in HF solution to reduce its diameter; (b) the end face of the fiber is then machined, via focused ion beam (FIB) milling, in the form of a ridge; (c) the ridge is then carved in the shape of a cantilever, equipped with a tip on its free hanging end; (d) a scanning electron micrograph (SEM) of the final cantilever.

Fig. 2. Schematic view of the experimental setup for the AFM imaging (not to scale). The probe was equipped with a sharp pyramidal tip, anchored to a translation stage consisting of a vertical piezoelectric actuator and an XY-scanner. Inset: scanning electron microscopy image of the tip of the cantilever. Scale bar: 2 μm.

Fig. 3. AFM images of the TGQ1 test grating (10 x 10 μm, 256 x 256 pixels.). (a) AFM image in air scanned from left to right; (b) overlay of scans from left to right and from right to left; (c) AFM image taken in water; (d) independent measurement in air, using a commercial AFM (NT-MDT). Line profiles show cross-sections at the position of the line.

Fig. 4. Schematic view of the experimental setup for indentation measurements. The fiber was attached onto a piezoelectric actuator, which was mounted, on an inverted microscope. The piezoelectric actuator was driven by a 2 Hz periodic triangular signal from a wave generator, as well as a fast oscillation from a lock-in amplifier. We measured both the output of the readout (S_{DC}) and the signal at the exit of the lock-in (S_{LI}).

Fig. 5. Measurement results of the indentation experiment in water. The output of the readout (S_{DC}), the signal at the exit of the lock-in amplifier (S_{LI}), the unitary circle obtained from S_{DC} and S_{LI}, and the extracted displacement from the phase of the unitary circle are shown from (a) to (d) respectively.

Fig. 6. Load-indentation curve extracted from the data reported in Fig. 5. The Young modulus of the sample can be derived from the pull out curve by means of the Oliver and Pharr method (Oliver & Pharr, 1992).

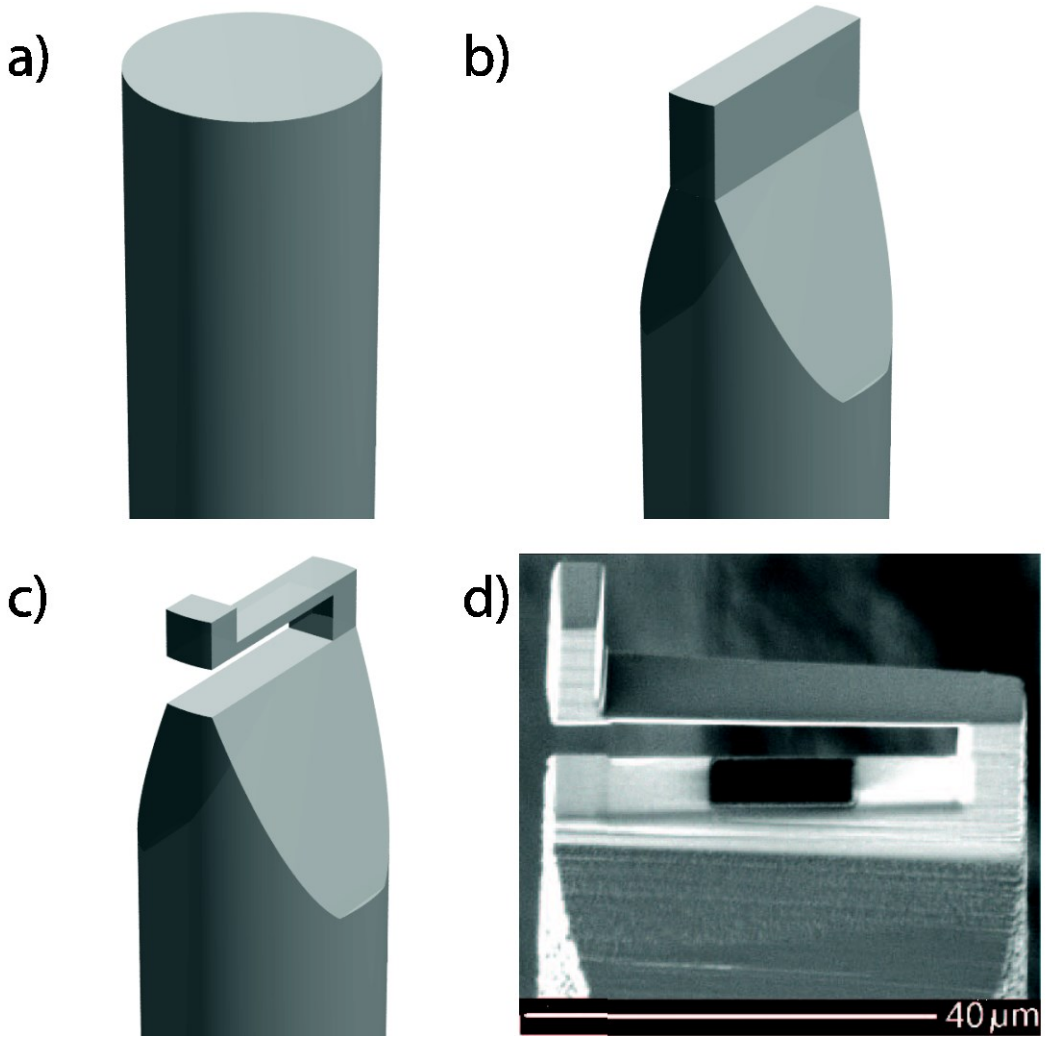
a)
b)
c)
d)
40 µm

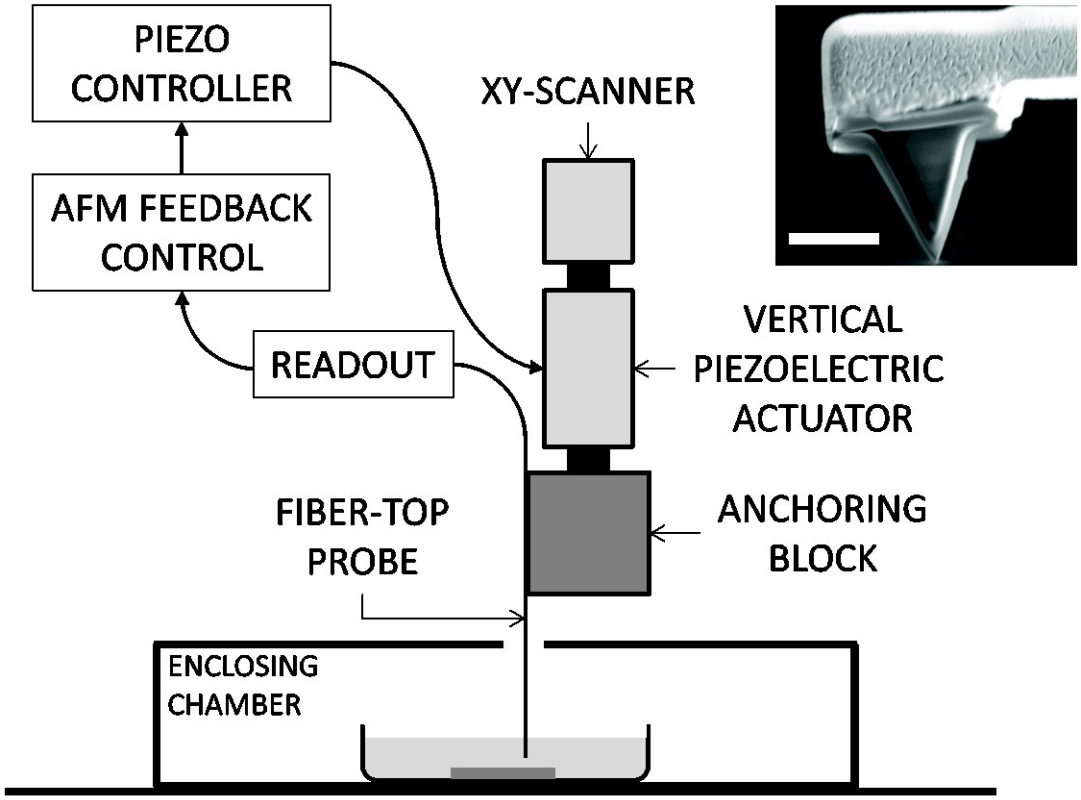
PIEZO CONTROLLER
AFM FEEDBACK CONTROL
READOUT
XY-SCANNER
VERTICAL PIEZOELECTRIC ACTUATOR
ANCHORING BLOCK
FIBER-TOP PROBE
ENCLOSING CHAMBER

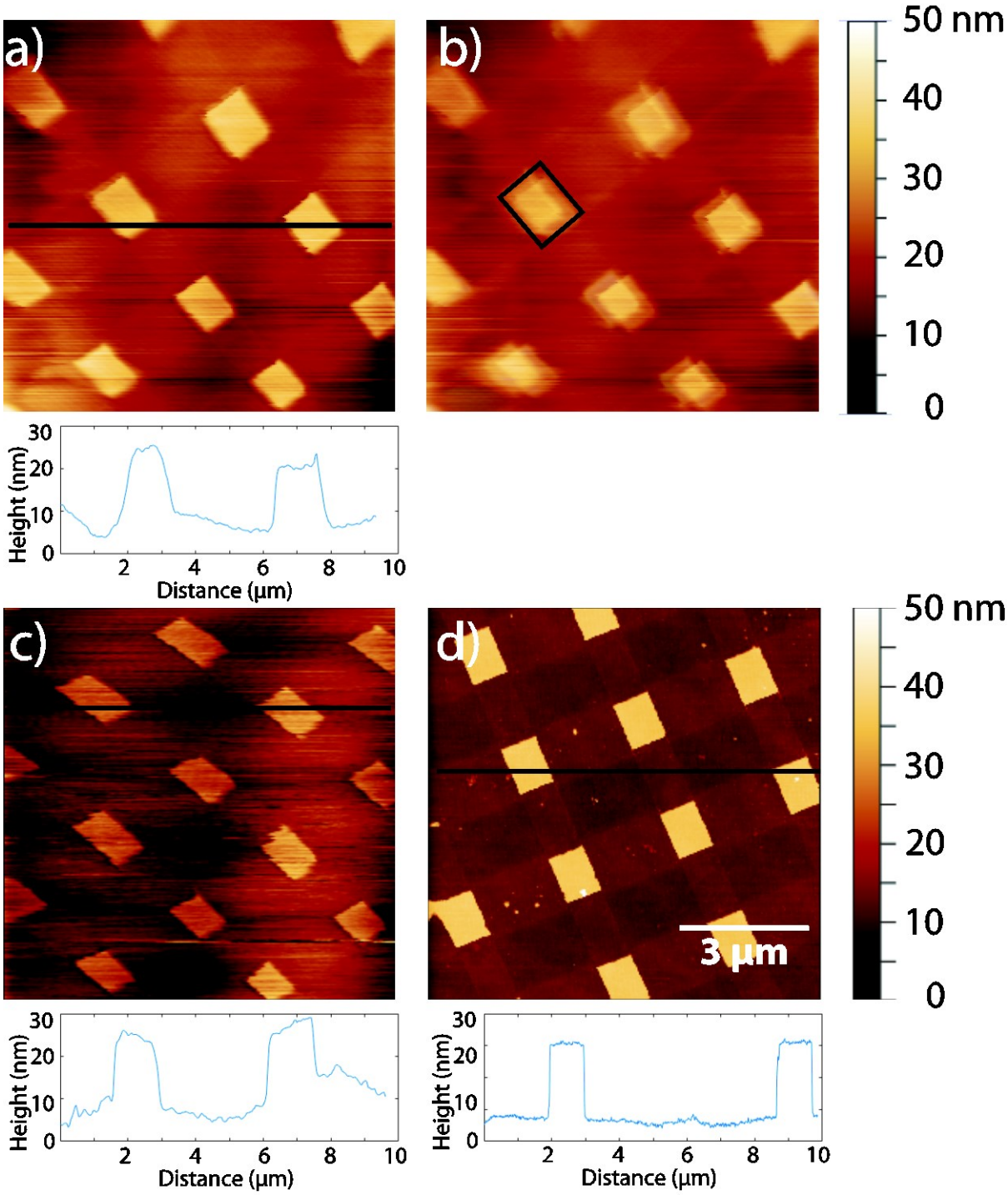
a)
b)
50 nm
40
30
20
10
0
Height (nm)
30
20
10
0
2
4
6
8
10
Distance (μm)
c)
d)
3 μm
50 nm
40
30
20
10
0
Height (nm)
30
20
10
0
2
4
6
8
10
Distance (μm)
Height (nm)
30
20
10
0
2
4
6
8
10
Distance (μm)

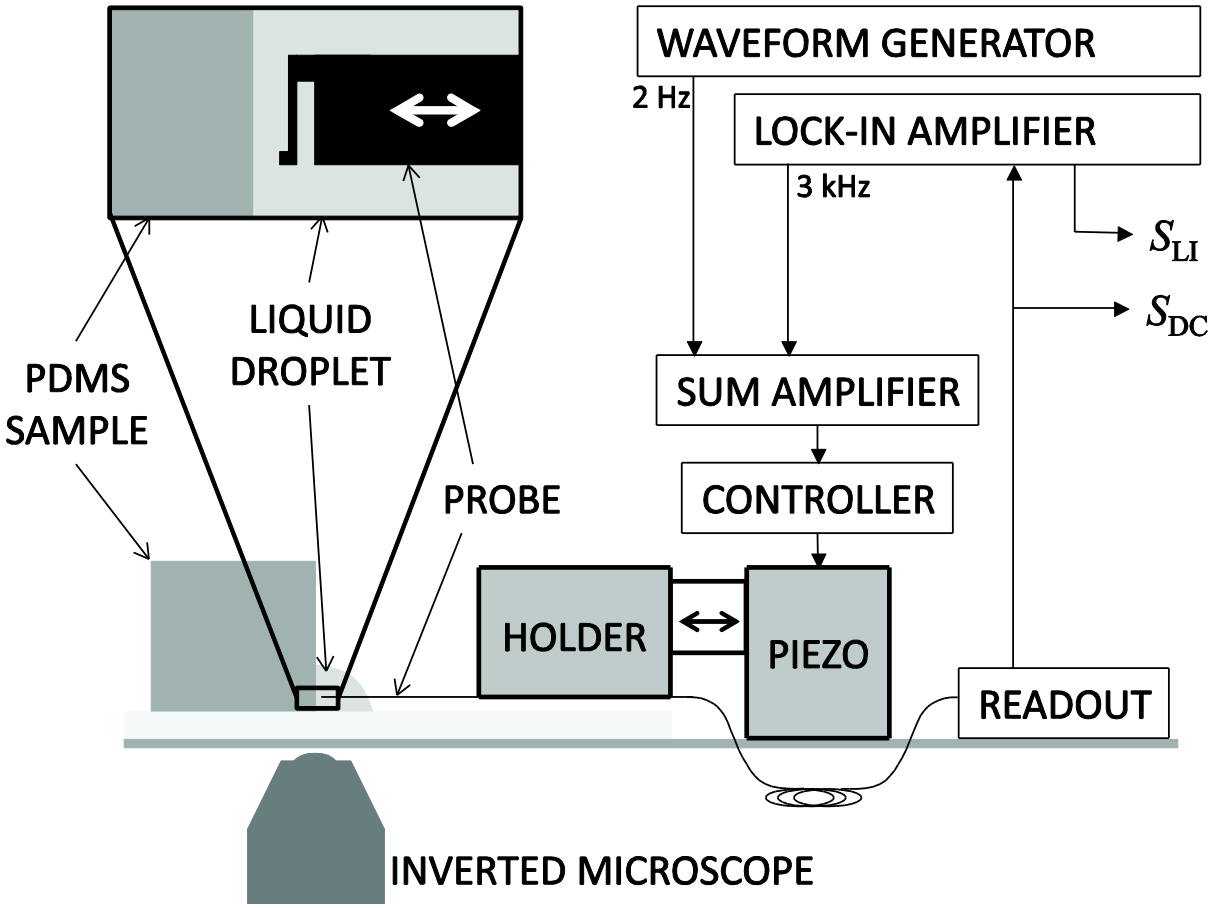
WAVEFORM GENERATOR
2 Hz
LOCK-IN AMPLIFIER
3 kHz
S_{LI}
S_{DC}
SUM AMPLIFIER
CONTROLLER
PIEZO
READOUT
HOLDER
PROBE
LIQUID
DROPLET
PDMS
SAMPLE
INVERTED MICROSCOPE

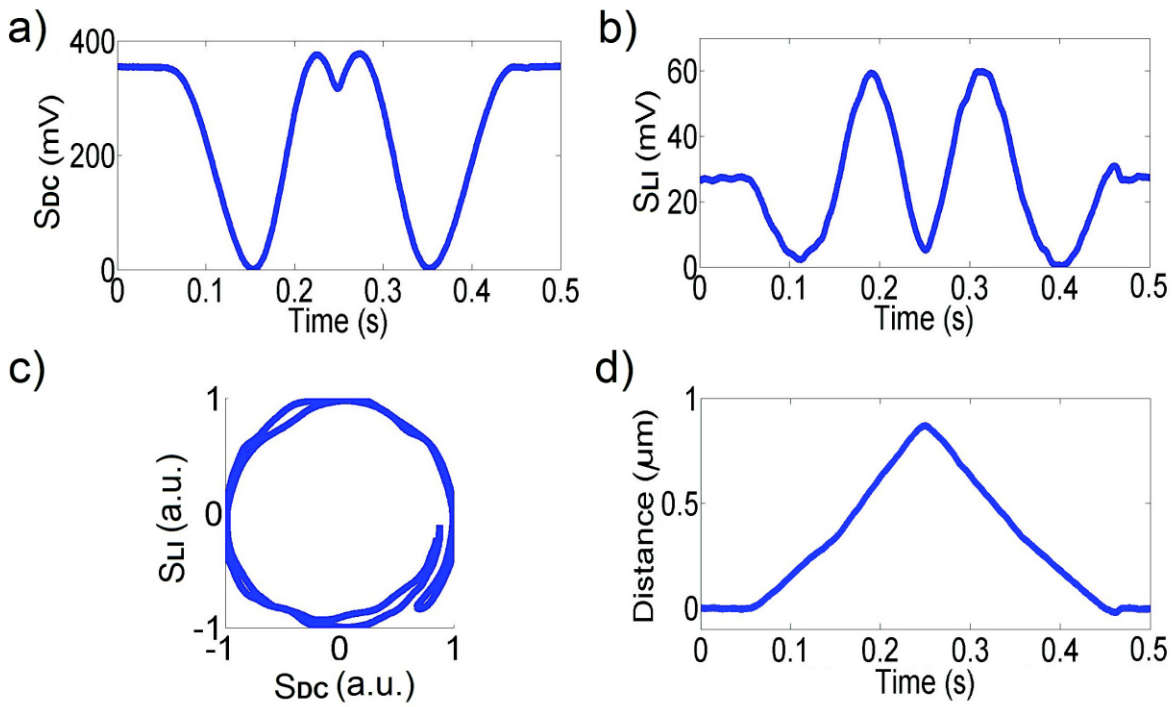
a)
400
200
0
S_{DC} (mV)
0
0.1
0.2
0.3
0.4
0.5
Time (s)
b)
60
40
20
0
S_{LI} (mV)
0
0.1
0.2
0.3
0.4
0.5
Time (s)
c)
1
0
-1
S_{LI} (a.u.)
-1
0
1
S_{DC} (a.u.)
d)
1
0.5
0
Distance (μm)
0
0.1
0.2
0.3
0.4
0.5
Time (s)

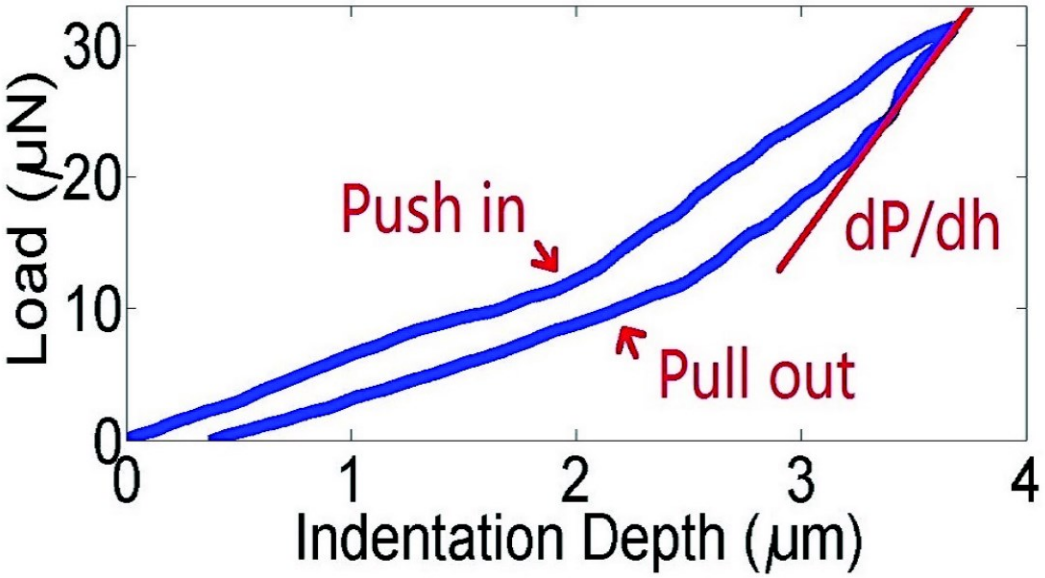
Load (μN)
30
20
10
0
0
1
2
3
4
Indentation Depth (μm)
Push in
Pull out
dP/dh